Published in final edited form as:
Prostate. 2008 September 15; 68(13): 1430–1442. doi:10.1002/pros.20807.

T40214/PEI Complex, a Potent Therapeutics for Prostate Cancer that Targets STAT3 Signaling

Priya Weerasinghe[1], **Yifei Li**[1], **Yongli Guan**[1], **Ruiwen Zhang**[3], **David J. Tweardy**[1,2], and **Naijie Jing**[1,2,*]

[1] Department of Medicine, Baylor College of Medicine, Houston, TX 77030

[2] Dan Duncan Cancer Center, Baylor College of Medicine, Houston, TX 77030

[3] Department of Pharmacology and Toxicology, University of Alabama at Birmingham, AL

Abstract

Background—Prostate cancer is the most common cancer among men in American and the second leading cause of cancer death. The treatment options employed for patients with advanced and metastatic prostate cancer are limited. As a critical mediator of oncogenic signaling, STAT3 is active in 82% of patients with prostate cancer. STAT3 has become a very important molecular target for prostate cancer therapy since it upregulates the oncogenes encoding apoptosis inhibitors, cell-cycle regulators, and inducers of angiogenesis. However, no anti-tumor drug whose primary mode of action is to target STAT3 has yet reached the clinic. To this end, we have laid the initial groundwork to develop the STAT3-inhibiting G-quartet oligodeoxynucleotide (GQ-ODN), T40214, for treatment of prostate cancers.

Methods—We employed *in vitro* and *in vivo* assays, including western blots, EMSA, cell cycle analysis, TUNEL and xenograft models, to determine the drug efficacy and mechanism of T40214/PEI complex.

Results—The results demonstrated that (i) T40214 significantly inhibited STAT3 activation and induced apoptosis in both androgen-dependent and androgen-independent prostate cancer cells; (ii) T40214 delivered by PEI (ployethylenimine) significantly suppressed prostate tumor growth in tumor-bearning nude mice due to that T40214 inhibited STAT3 activation and then greatly promoted apoptosis, reduced angiogenesis and cell proliferation in prostate tumors.

Conclusion—Our studies suggested that STAT3 is a critical oncogenic signal, which strongly influences the progression of prostate cancers and that T40214/PEI complex is a promising candidate for treatment of patients with prostate tumors and represents a novel strategy for prostate cancer therapy.

INTRODUCTION

Prostate cancer is the most frequently diagnosed cancers among men in the United States and the second leading cause of cancer death (1). Although the etiology of prostate cancer is not well understood, androgens and androgen receptors have been shown to play a critical role in prostate tumorigenesis. Prostate cancer initially occurs as an androgen-dependent tumor, and most patients respond to androgen–ablation therapy. However, the disease often recurs as an androgen–independent tumor, which is no longer sensitive to the ablation treatment. In the case of recurrence, treatment consists of cytotoxic chemotherapeutic

Corresponding Author: Naijie Jing, Ph.D.*, Department of Medicine and Cancer, Center Baylor College of Medicine, One Baylor Plaza - N520, Houston, Texas 77030 USA, Tel: 713-798-3685, Fax 713-798-8948, Email: njing@bcm.tmc.edu.

agents, which have formidable nonspecific cytotoxic effects, that frequently produce undesirable side effects. Additionally, androgen-independent prostate tumors do not respond well to chemotherapeutic agents, resulting in a poor prognosis for patients (2). Therefore, developing novel therapies, including novel molecular targets and new agents with different therapeutic mechanisms of action, will be needed to cure prostate cancer patients.

Signal transducer and activator of transcription (STAT) 3, a member of the STAT protein family, is constitutively activated in many different tumors, including hematological and solid tumors (3). Upon phosphorylation tyrosine kinases, STAT3 tail-to-tail dimerization and translocates to the nucleus, where it binds to the specific promoter sequences, thereby modulating expression of specific downstream genes. STAT3-related downstream genes have essential functions in signaling pathways critical to normal cellular processes such as differentiation, proliferation, survival, development and immune function (3–5). Constitutive STAT3 activation was observed in 82% of prostate tumors, indicating that STAT3 was activated in the tumor cells of prostate cancer. In additional, STAT3 activated by interleukin-6 (IL-6) was overexpressed in prostate cancer cells, including both androgen-dependent and androgen–independent cells (6). IL-6 activation of JAK/STAT3 pathway was accompanied by transition from androgen-sensitive to androgen-insensitive prostate cancer cell growth (7). IL-6 also activated androgen receptor (AR)-dependent gene expression in prostate cancer cells in the absence of androgen (8). Although the role of STAT3 in prostate cancer is not clearly established, activated STAT3 is considered to be an important signaling molecule that plays a critical role in progression of both androgen-dependent and -independent prostate cancers (9,10).

Recently, we developed a G-quartet oligodeoxynucleotide (GQ-ODN) that is a potent STAT3 inhibitor, for cancer therapy (11,12). GQ-ODNs are composed of G-rich DNA sequences, which have been identified, cloned, and characterized in the telomeres of many organisms (e.g., fungi, ciliates, vertebrates, and insects) (13). G-quartets stack on top of one another, creating tetrad-helical structures and forming a family of structures that includes folded G-quartets produced by intramolecular interactions, as well as hairpin dimers and parallel-stranded tetramers resulting from intermolecular interactions. In general, G-quartet structures are very stable; however, their stability depends on the presence of monovalent cations and a concentration of G-rich oligonucleotides, especially for dimer or tetramer formation (14–17). The principal difficulty in delivering GQ-ODNs to cells arises from the physical and structural properties of the GQ-ODN (18). Because of their large molecular size and charge, GQ-ODNs cannot directly penetrate cell membranes. Based on the mechanism by which potassium ions induced the formation of the G-quartet structure, we have developed a novel delivery system for our GQ-ODN that can increase drug delivery efficiency and activity *in vitro* and *in vivo* (18–20) To this end, we have laid the initial groundwork to develop GQ-ODN T40214, which forms G-quartet helical DNA structures, as a potent inhibitor of STAT3 activation (19,20). T40214 as a biologic agent composed of 16-mer oligonucleotide, $(GGGC)_4$, forms a stable G-quartet motif (21,22), which prevents single-strand endonucleases from accessing their cleavage sites, leading to a long oligonucleotide half-life in serum and inside cells. This motif significantly increases the ability of nuclease resistance and its long-term biological efficacy (23). Also, G-rich oligonucleotide was identified as low toxicity agents previously (24). In this report, we demonstrate that (i) T40214 delivered by PEI (ploy ethylenimine) induces apoptosis in both androgen-dependent and androgen-independent prostate cells by targeting STAT3; (ii) based on our effective delivery system, T40214 significantly suppresses prostate tumor growth and greatly increases the survival of tumor-bearning nude mice, indicating that T40214/PEI complex is a promising candidate for further development as a novel treatment for prostate cancer.

MATERIALS AND METHODS

Materials

The following polyclonal antibodies were obtained from Santa Cruz Biotechnology, Inc. (Santa Cruz, CA): anti-STAT3; anti-Stat1; anti-cyclin D1 against amino acids 1–295, which represents full-length cyclin D1 of human origin; anti-VEGF; anti-Bcl-xL; and anti-Bcl-2. Phospho-specific antibodies, p-STAT3, were purchased from Cell Signaling Technology (Beverly, MA). Goat anti-rabbit horseradish peroxidase (HRP) conjugate was purchased from Bio-Rad Laboratories (Hercules, CA), goat anti-mouse HRP conjugate was purchased from BD Transduction Laboratories (Lexington, KY). Penicillin/Streptomycin, RPMI-1640 medium, fetal bovine serum (FBS), and 0.4% trypan blue vital stain were obtained from Invitrogen Corporation/Life Technologies, Inc. (Grand Island, NY). Oligonucleotides: T40214 with the sequence of GGGCGGGCGGGCGGGC and ns-ODN with the sequence of TGCCGGATGAAGAGCTACCA were synthesized and purified by The Midland Certified Reagent Company, Inc. (Midland, TX), Polyethylenimine (PEI, Mw ~25,000) was purchased from Aldrich Chemical, WI.

Cell Lines and Cell Culture

The cell lines used in our studies included: PC3, DU145 and LNCaP, which were purchased from ATCC (Manassas, VA). These cell lines were cultured in DMEM medium supplemented with 10% FBS, 100 units/ml penicillin, and 100 μg/ml streptomycin and maintained in 37°C incubator. GQ-ODN T40214 was mixed with PEI at the ratio of 1:2. The T40214/PEI mixture was added to the 6-well plates (about $6–9\times10^5$ cells/well) after the cells were seeded. The dose of T40214 added in 6-well plate were: 0, 0.7, 7.0, 14 and 70 μM. After incubation for 3 hrs in the incubator, cells were washed three times with fresh medium without FBS and continue to incubate for 24 hrs and then followed by protein extraction for western blot analysis to determine the drug activity.

Western Blot Analysis

To determine the effect of GQ-ODN T40214 on STAT3 phosphorylation, cytoplasmic extracts were prepared from murine tumor tissue or prostate cancer cells that had been pretreated with T40214/PEI, as previously described . Prostate cancer cells (1 million cells of LNCaP and DU145 cells and 8 million cells of PC3 cells, due to low expression of STAT3 in PC3 cells) were first stimulated with IL-6 (25 ng/ml) for 30 minutes. Cells were then washed in serum-free medium and incubated with various concentrations (0.7–70 μM) of T40214/PEI complexes for 24 hours. Cells were lysed with cell lysis buffer and 30 micrograms of whole cell protein was resolved on 10% SDS-PAGE gel, transferred to a nitrocellulose membrane, blocked with 5% nonfat milk, and probed with specific antibody against STAT3 and tyrosine-phosphorylated STAT3 (p-STAT3). Xenografted tumors were harvested at the end of treatment, diced into small pieces, and sonicated on ice for 2 minutes. Tumor tissue (100 mg) was lysed in 300 μl of lysis buffer containing protease and phosphatase inhibitors. Tumor tissue protein (50 μg) was resolved on SDS-PAGE gel and probed by specific antibodies, as previously described. The bands were quantitated using a Personal Densitometer Scanner (version 1.30) and ImageQuant software (version 3.3) (GE Healthcare/Amersham Biosciences).

Electrophoretic mobility shift assay (EMSA)

EMSA was performed, as previously described (19). Briefly, IL-6 (25ng/mL) was added into wells containing $5–7\times10^5$ prostate cancer cells. Cells were washed and extracted using high-salt buffer. The protein concentrations of the extracts were determined using a Bradford assay (Bio-Rad Laboratories). The ^{32}P-labeled duplex DNA probe (hSIE, 5′-

AGCTTCATTTCCCGTAAATCCTA) was purified using G-25 columns (GE Healthcare/ Amersham Biosciences). Labeled hSIE probe was mixed with 5μg of cell protein in 1x binding buffer and 2μg of poly-dIdC, and incubated at room temperature for 15 minutes, with or without GQ-ODN. Samples were loaded onto 5% polyacrylamide gel containing 0.25 x TBE and 2.5% glycerol. The gel was run at 160–200 V for 2–3 hours at room temperature, dried, and autoradiographed.

Non-denatured DNA electrophoresis

5′-end labeling of the oligos: 200ng of each oligo; 5ul of reaction buffer containing: 350 mM Tris-HCl (pH 7.6), 50mM MgCl2, 500 mM KCl and 5 mM 2-mercaptoethanol; 2ul of r-^{32}P-ATP (10uCi/ul, 3000 Ci/mmol, from Amersham Biosciences) and 10 units of T4 Polynucleotide Kinase (Invitrogen, Carlsbad, CA) in a total reaction volume of 25ul, incubated at 37°C for 30 min, then added to MicroSpin G-25 Columns (Amersham Biosciences) to purify the end-labeled T40214. About 80ng of labeled oligos were loaded in a 20% non-denatured polyacrylamide gel. The gel was run at 150V for 4 hr in cold room (4°C) and autoradiographed.

Cell cycle analysis

PC3, DU145 and LNCap cells treated with T40214/PEI, PEI or ns-ODN/PEI (nonspecific oligodeoxynucleotide) were harvested using 0.25%tripsin EDTA (Invitrogen CA), washed with PBS and fixed with ice cold 70% ethanol (0.5 ml) at 4°C overnight. The fixed cells were washed twice with ice cold PBS and re-suspended in 0.25 ml PBS containing 5 μl of 10 mg/ml Rnase (Sigma). The cells then were incubated at 37 °C for 1 hour and stained with 10 μl of 1 mg/ml propidium iodide (Sigma). Then the cells were analyzed by FACS using a Becton Dickinson flowcytometer (Rutherford, NJ). Histogram plots were created using CellQuest program (Beckton Dickinson, San Jose CA). Percentages of cells within the various phases of cell cycle were calculated using CellQuest by gating G_0/G_1,S and G_2+M cell populations.

Detection of mitochondrial membrane potential

Using three different prostate cancer cell lines, PC3, DU 145 and LNCap $\Delta\Psi$ were determined by accumulation of the cataenic fluorechrome that accumulates differently in healthy vs apoptotic cells. After overnight drug treatment, cells were tripsinized, washed then mitochondrial integrity was assayed by using "Mitocapture™ Mitochondrial Apoptosis Detection Kit" (BioVision, Mountain View, CA). Briefly, each unfixed cell sample was washed with PBS, incubated with the Mitocapture reagent for 20 min at 37 °C in a 5% CO2 incubator. The cells were then washed, counted, 10,000 cells were analyzed using a FACS Calibur flowcytometer. Data analysis was performed with CellQuest software.

TUNEL Analysis

Tissue sections (5 μm) were mounted on siliconized glass slides, air dried, and heated at 45°C overnight. After deparaffinization and rehydration, the sections were digested with proteinase K (120μg/ml) for 20 minutes at room temperature. Following quenching of the endogenous peroxidase activity, the sections were washed in PBS, and subsequently incubated with equilibration buffer for 10 minutes at room temperature. Sections were boiled and 50 μl of a mix containing terminal deoxynucleotidyl transferase, reaction buffer containing dATP, and digoxigenin-11-dUTP was then added. The sections were covered with a plastic coverslip, washed in stop/wash buffer for 10 minutes at room temperature, and subsequently washed in PBS. The sections were then incubated with anti-digoxigenin peroxidase for 30 minutes at room temperature and washed in PBS. Color development was accomplished through immersion of the slides in 3′3 diaminobenzidine/0.1% H_2O_2 for 3–7

minutes. Sections were counterstained with ethyl green, washed in butanol, cleared in xylol and mounted with permount.

In vivo drug tests

(i) Establishing the nude mouse xenograft model for in vivo testing—Athymic nude mice (Balb-*nu/nu*, 4–5 weeks old, weighing approximately 20g) were ordered from Charles River Laboratories, Inc. (Wilmington, MA). Approximately 2.5 ~ 4.0 million cancer cells in 200 μl of PBS were then injected subcutaneously into the right flank of each mouse.

(ii) Continue drug treatment—After tumors were established (50–150mm^3), the nude mice were randomly assigned to several groups: The mice in Group 1 were not treated, and were used as controls; Group 2 received placebo treatment with PEI (2.5 mg/kg) alone; Group 3 was treated with ns-ODN/PEI (10mg/kg+2.5mg/kg) as a control ODN; Group 4 was treated with T40214 without PEI (10mg/kg); Group 5 was treated with paclitaxel (10mg/kg), a clinic drug as positive control; Groups 6 and 7 were treated with T40214/PEI at doses of 5mg/kg+1.25mg/kg and 10mg/kg+2.5mg/kg, respectively. Each group was composed of 5 mice. The the mice of each group were continually treated by intraperitoneal (IP) injection every other day for 3–4 weeks. Body weight and tumor size were measured every other day. Tumor size was calculated using the function (a x 0.5b^2), where *a* equals the length and *b* equals the width of tumors.

(iii) Cyclic drug treatment—After the PC-3 tumors reached 50–150mm^3, the mice were randomly divided in three groups: Group1 was placebo treated with PEI (2.5 mg/kg) alone; Group2 was treated with ns-ODN/PEI (10mg/kg+2.5mg/kg); and Group3 was treated with T40214/PEI (10mg/kg+2.5mg/kg). The mice were treated with 5 times/week during weeks 1 and 3, and did not receive treatment during weeks 2 and 4.

(iv) The T40214/PEI complex—Dissolved T40214 in H_2O was heated at 95°C for 10 minutes and gradually cooled to room temperature. The oligo was checked by OD to count ODN concentration. Then PEI was added into T40214 solution to make the complex of T40214/PEI at 1μg/μl of ODN with 0.25μg/μl of PEI. The amount of drugs was given based upon the body weight of each mouse, which was measured at each injection.

RESULTS

We have previously shown that GQ-ODN T40214, which forms an intramolecular G-quartet structure (Fig. 1A) (18,21,22), significantly inhibited the growth of xenograft tumors, including SCCHN and NSCLC, in nude mice by inhibiting STAT3 activation (25,26). In order to develop T40214 as potential agent for prostate cancer therapy, we have performed further *in vitro* and *in vivo* studies of T40214 to demonstrate its efficacy in models of prostate cancer.

T40214 inhibits STAT3 DNA-binding activity in prostate cancer cells

Effective intracellular delivery is essential for the success of cancer therapeutics targeting STAT3. Recently, we developed an intracellular delivery system for GQ-ODN, in which we used PEI as a vehicle to deliver T40214 into cells. Once T40214 was inside the cells, the G-rich T40214 formed G-quartet structures which can penetrate the cell nucleus through nuclear pores. A non-denatured polyacrylamide gel (Fig. 1B) showed that the free T40214 (Lane1) corresponds to a G-quartet structure. T40214 with PEI (Lane2) results in two bands, indicating that a portion of the ODNs adhered to cell membranes (the upper band), and a portion of the ODNs entered into the cells (the lower band) after the T40214/PEI complexes were incubated with cancer cells for 24 hrs. Since the same migration pattern was observed

for free T40214, the T40214 inside the cells was concluded to have formed G-quartet structures. Analysis of the band intensities indicated that about 72% of T40214 is delivered successfully. In the absence of PEI (Lane3), T40214 only produced a single band higher on the gel, demonstrating that T40214 itself cannot directly enter into the cells due to its large molecular size and charge.

To determine the mechanism by which T40214 inhibits STAT3 activation in prostate cancer cells, both western blot assays and EMSA were performed. Western analysis showed that, compared with the expression of phosphorylated STAT3 (p-STAT3) in cells exposed to ns-ODN/PEI (non-specific ODN as control), the cells exposed to T40214 (14μM) exhibited mild suppression of p-STAT3 expression in all three prostate cancer cell lines (Fig. 1C). Since the expression of STAT3 in PC3 cell line was much lower than in DU145 and LNCaP cell lines, the PC3 cells used in the western blot was 8 times more than DU145 and LNCaP cells. However, EMSA studies (Fig. 1D) demonstrated that the delivery of T40214 strongly inhibited STAT3 DNA binding activity in both androgen-dependent (LNCaP) and androgen-independent (PC-3) prostate cancer cells. These results suggest that T40214 mainly inhibits STAT3 activation in prostate cancer cells by blocking p-STAT3 DNA binding activity.

T40214 induces apoptosis and arrests cell proliferation in prostate cancer cells

To determine whether T40214 arrests cell proliferation and promotes apoptosis through inhibiting STAT3 activation, cell cycle analyses were performed in both androgen-dependent (LNCaP) and androgen-independent (DU145 and PC-3) prostate cancer cells. The histograms of cell cycle distribution in prostate cancer cells (LNCaP, DU145 and PC-3) were determined using propidium iodide (PI)/flow cytometry. Cells in the sub-G1 (SG1) phase generally have DNA damage associated with cell death. The histograms demonstrated that the percentage of cells in SG1 in all three cancer cell lines was not changed by treatment with PEI alone or with ns-ODN/PEI (non-specific ODN as a control) (Fig. 2A). However, in the LNCaP, DU145 and PC-3 cells exposed to T40214/PEI, the percentage of cells in SG1 increased from 1.7% to 19.2%; from 0.8% to 16.1%; and from 1.4% to 45.5%, respectively, showing that T40214 significantly increased cell apoptosis in the three prostate cancer cells. In addition, the number of cells in the G2 phase decreased from 19.5% to 16.4%; from 26.2% to 22.0%; and from 26.6% to 12.1%, for the LNCaP, DU145 and PC-3 cells, respectively. This demonstrates that the proliferation of the three cancer cell lines was also arrested by T40214, and that the PC-3 cells were especially sensitive to the effects of T40214.

GQ-ODN causes a decrease in mitochondrial membrane potential

Before cells exhibit common signs of nuclear apoptosis (chromatin condensation and endonuclease-mediated DNA fragmentation), they undergo a reduction of the mitochondrial transmembrane potential. Fig 2B shows a clear reduction of mitochondrial potential in PC3 prostate cancer cells treated with T40214/PEI, while an overwhelming majority of cells in the control cell populations exhibited normal levels of mitochondrial potential (over 90 %). Thus, treatment of cells with T40214/PEI resulted in 39.6% cells with reduced mitochondrial potential; among the control groups, only 8.4% of untreated control cells, 6.4% of cells treated with PEI alone and 8.5% of ns-ODN/PEI treated cell showed any reduction in mitochondrial transmembrane potential. The low levels of apoptosis encountered among the control groups can explain their relatively smaller reductions in mitochondrial potential. Conversely, higher levels of apoptosis found in the T40214/PEI treated cell group accounted for their greater reduction in mitochondrial potential, matching the observation in cell cycle analyses (Figure 2A). Furthermore, we also investigated the effects of drug treatment on the mitochondrial membrane potential in two other prostate cancer cell lines: LNCaP and DU145. The treatment of prostate cancer cells with T40214/

PEI showed that the mean percentages of mitochondrial potentials in cells were reduced to 32% in LNCaP cells and to 24% in DU145 cells, respectively (Fig. 2C). Together, increase of the percentage of cells in SG1 and decrease of the reduction in mitochondrial potential provided evidence that T40214/PEI complex significantly induced apoptosis in all three prostate cancer cells.

T40214 significantly suppresses the growth of prostate tumor xenograft in nude mice

To investigate its *in vivo* activity, we evaluated the effects of T40214 against a xenograft model of prostate cancer (PC-3).

Determination of the effects of T40214 against prostate cancer—We found that over the 24-day treatment period, the mean size of prostate xenograft tumors in the untreated (Group 1); the placebo-treated (Group 2) and ns-ODN-treated (Group 3) mice increased from 93 to 2633 (mm^3); from 58 to 1924 (mm^3); and from 68 to 2362 (mm^3), respectively. The mean size of tumors in the paclitexal-treated mice (Group 5) increased from 71 to 672 (mm^3). The mean size of tumors in the T40214-treated mice (Group 4) increased from 56 to 1327 (mm^3); however, the mean sizes of tumors in the T40214/PEI-treated mice in Group 6 increased only from 73 to 329 (mm^3) and the T40214-treated mice in Group 7 actually demonstrated a decrease in tumor size, from 91 to 55 (mm^3) (Table 1, *p* Figs 3 and 4). When compared with untreated animals (mean weight of tumors was 1.37 ± 0.37g), neither PEI nor ns-ODN had any appreciable effect on tumor growth. Paclitaxel had a growth inhibitory effect (0.47 ± 0.22g) and T40214/PEI significantly suppressed the growth of prostate xenograft tumors in nude mice (mean weight of tumors: 0.18 ± 0.10g, =0.02). We also found that when T40214 was delivered by PEI, it led to significant suppression of tumor growth in all of the mice in Groups 6 and 7, with more potent effects being observed in the group receiving the higher dose. When T40214 was administered alone, only about one out of five mice demonstrated drug effects on the growth of their tumors (Fig. 3B, Line 4), indicating that the PEI delivery system was essential for drug efficacy *in vivo*.

Drug efficacy in cyclic treatment—To determine the duration of the anti-cancer effects of GQ-ODN T40214, we injected the compounds 5 times/week following cycles of one week on and one week off for a month. We found (Fig. 4E) that compared with the control groups (1 and 2), the tumor growth of T40214/PEI-treated mice (Group 3) was suppressed during the weeks the mice were not treated, suggesting that GQ-ODN T40214 has long-term therapeutic activity against prostate cancer.

Effect of T40214/PEI treatment on survival—To determine whether or not T41214/PEI treatment reduced mortality of nude mice harboring prostate tumor xenografts, we performed survival studies in which animals were sacrifice when they were moribund or their tumor reached a volume of 1,000 mm^3 or at day 24. The time point at which 50% of the mice remained alive (50% survival point; Fig. 4D) in the untreated, placebo-treated and ns-ODN-treated mice was 7, 12 and 10 days, respectively. Paclitaxel treatment extended the 50% survival point to 18 days. However, the 50% survival point for both T40214/PEI-treated mice was ≥ 24 days with 100% of the mice in the 10 mg/kg group surviving to 24 days. Thus, T40214/PEI complex as a therapeutic agent significantly increased the survival time of the mice with androgen-independent prostate tumors.

The mechanism of T40214 suppressing the prostate tumor growth

To determine the mechanism by which T40214 suppresses tumor growth, we employed western blot and TUNEL assays of tumor tissues which were harvested from the mice at the end period of drug treatments. First, we used one sample of untreated tumors as a control (Group1) and two samples of PEI-, ns-ODN and T40214-treated tumors from Groups 2, 3

and 6, respectively, to perform immunoblotting assays. Since equal amounts of protein were loaded for each tumor sample, the results demonstrate that STAT3 proteins were constitutively phosphorylated in androgen-independent prostate tumors (PC-3) and that the activation of p-STAT3 in the tumors was totally inhibited by the T40214/PEI complex at the 5mg/kg+1.25mg/kg dose (Fig. 5A). In addition, delivery of T40214 completely inhibited the expression of p-STAT3 down-stream proteins, including Bcl-2, VEGF, and Cyclin D1 in the prostate tumors.

Finally, the TUNEL assay, which labels the apoptotic cells with cleaved DNA fragments, was performed to determine at the single cell level the extent of apoptosis in the T40214/PEI-treated prostate tumors. The TUNEL-positive apoptotic tumor cells were stained dark as observed by light microscopy, while the non-apoptotic cells appeared in blue. There was significant apoptosis in the T40214/PEI-treated tumor (Fig. 5B). Upon examination of the number of apoptotic cells within the total cell population in the tumors, we noted that the mean percentage of apoptotic cells in placebo-treated tumors were 10±5% and that in T40214-treated mice was 80±5%.

DISCUSSION

Previous *in vitro* studies have shown that IL-6-induced activation of STAT3 is accompanied by a transition from androgen-sensitive to androgen-insensitive growth of prostate cancer cells (7). Moroever, the level of STAT3 activation in androgen-independent prostate cancer cells (PC-3 and DU145) is much higher than in androgen-dependent prostate cancer cells (LNCaP) (8). The formation and activation of STAT3 dimers in LNCaP cells by IL-6 led to an increase in free androgen receptor (AR), suggesting that activated STAT3 is an important signaling molecule involved in the induction of AR-mediated gene activation by IL-6, and that it plays a role in the progression of prostate cancer cells (9). We have demonstrated that T40214 strongly inhibits DNA binding p-STAT3 dimers and blocks its transcription in both androgen-dependent and –independent prostate cells (Fig. 1D). As a result of this inhibition, T40214 led to a significant induction of apoptosis and arrested cancer cell proliferation in three different prostate cancer cell lines (Fig. 2A). We have also shown that when T40214 was delivered using PEI, it significantly suppressed prostate tumor growth in animals by reducing p-STAT3 levels and triggering apoptosis of tumor cells (Figs 4 and 5). These results provide evidence to suggest that activated STAT3 is one of the key molecules that influences the growth of both androgen-dependent and –independent prostate cancer cells. Also, we found that STAT3 protein expression was low in PC3 cell line; however, p-STAT3 protein was readily detected in PC3 tumors grown in nude mice, suggesting that STAT3 is highly activated in the tumor environments. Targeting STAT3 signaling represents a novel and promising strategy for prostate cancer therapy.

STAT3 has been identified as a critical oncogenic signaling molecule, and plays pivotal roles in tumor promotion by up-regulating its target genes, which are involved in apoptosis (Bcl-x_L, Bcl-2, Mcl-1, and survivin), angiogenesis (VEGF), and cell proliferation (cyclin D1 and c-*myc*) (3). STAT3 and Stat1 have similar functional domains and also both form hemo- and heterodimers when activated. Protein sequence analyses have shown that Stat1 and STAT3 have 51%, 60% and 66% identity in the full length protein, SH2 domain and DNA-binding domain, respectively, which makes the selective inhibition of STAT3 a challenge. However, based upon the crystal structure of the STAT3 dimer (27) and experimental evidence (25), we made extensive use of computational studies to ensure that T40214 selectively targets STAT3 (28). In fact, we have demonstrated that GQ-ODN T40214 selectively inhibits STAT3 activation, but not the activation of other STATs (e.g. Stat1 and Stat5) or JAK kinases in both cell lines and tumors (26). The selective targeting of STAT3 is key to the design of a potent anti-cancer agent that will have fewer side-effects. This

specificity is expecially important since Stat1, which has such high homology to STAT3, acts in a pro-apoptotic and anti-proliferative manner, and its functions are in opposition to STAT3 (3).

Our studies of delivery (Fig. 1B) showed that GQ-ODN cannot directly enter cells, indicating that an effective delivery system is essential for the success of the agent in further in vivo and eventual clinical studies. An effective delivery system using PEI as vehicle for T40214 was established previously *in vitro* (12). The delivery system includes two main steps: (i) G-quartets with a neutral charge on the surface incorporate poorly into cationic vehicles. Electrostatic interactions are the primary driving force responsible for forming the GQ-ODN/vehicle complexes. Thus, the G-rich oligos need to be heated and denatured into random coils in order for them to incorporate with the vehicle. The T40214/PEI complex was formed by mixing the denatured T40214 possessing negative charges with PEI, which is positively chargerd. The positive charges in the surface of the T40214/PEI complexes enhance their cellular uptake. (ii) G-quartet formation strongly depends on the presence of cations, especially potassium. Generally, the potassium concentration is 4mM outside cells and 140mM inside cells. T40214 was designed to form a G-quartet in ~50mM KCl. Thus, T40214 molecules maintain their unfolded structure before entering cells. Once delivered into cells, T40214 forms a G-quartet structure inside cells at high K^+ concentration, and then it is able to penetrate into the nucleus through nuclear pores, as shown in Fig 6. PEI facilitates the delivery of T40214 to target cells for endocytosis, but PEI itself cannot enter into cells due to its positive surface charges.

Herein, we have demonstrated that the system successfully delivered up to 72% of the administered T40214 into cancer cells, and significantly increased its efficacy *in vivo*. When the prostate tumors were treated by T40214 alone, only one of five mice (~20%) demonstrated reduced growth of their tumors (Fig. 3B, Line 4). However, the growths of prostate tumors in the all five mice in Groups 7 treated with T40214/PEI were significantly suppressed (Fig. 3B, Line 7). Therefore, it appears that the T40214/PEI complex represents a promising candidate for prostate cancer therapy. The complex formed by T40214/PEI led to much stronger anti-tumor effects (p=0.0002) than paclitaxel (p=0.004), and the T40214/PEI complex treatment substantially prolonged the survival time of animals. G-rich oligonucleotides have previously shown low toxicity (29). In our study, after mice had been treated with T40214/PEI for 24 days, their mean body weights had increased by about 5%, indicating that T40214/PEI complex is well tolerated. We have also examined the duration of action of T40214/PEI and the results indicate that T40214/PEI has long-term anti-cancer efficacy (Fig. 4E), decreasing tumor growth even during “recovery” periods when the drug was not administered. Moreover, T40214/PEI also still was able to exert potent anti-cancer activity after treatment had been halted.

Cumulatively, our results indicate that we have established a system that specifically and effectively targets the STAT3 signaling pathway via GQ-ODN T40214, and that it appears to be appropriate for the treatment of both androgen-dependent and –independent prostate cancers. These pre-clinical results demonstrated that the T40214/PEI complex represent a novel and potent anti-cancer agent that significantly suppresses the growth of prostate xenograft tumors. The results also provide useful information for developing a novel strategy for treatment of cancer. This is timely since innovative treatments employing new agents, especially those with different mechanisms of action and novel molecular targets, are urgently needed for human cancer therapy. We believe that the results provide evidence to support testing of the 40214/PEI complex in future clinical studies.

Acknowledgments

This work was supported by NIH CA104035 and Competitive Award from Prostate Cancer Foundation (NJ).

References

1. Jemal A, Siegel R, Ward E, et al. Cancer statistics, 2007. CA Cancer J Clin. 2007; 57:43–66. [PubMed: 17237035]
2. Edwards J, Bartlett JM. The androgen receptor and signal-transduction pathways in hormone-refractory prostate cancer. Part 2: Androgen-receptor cofactors and bypass pathways. BJU Int. 2005; 95:1327–35. [PubMed: 15892826]
3. Yu H, Jove R. The STATS of cancer-new molecular targets come of age. Nature Rev/Cancer. 2004; 4:97–105.
4. Bowman T, Garcia R, Turkson J, Jove R. STATs in oncogenesis. Oncogene. 2000; 19:2474–2488. [PubMed: 10851046]
5. Buettner R, Mora LB, Jove R. Activated STAT signaling in human tumor provides novel molecular targets for therapeutic intervention. Clin Cancer Res. 2002; 8:945–954. [PubMed: 11948098]
6. Mora LB, Buettner R, Seigne J, Diaz J, Ahmad N, Garcia R, Bowman T, Falcone R, Fairclough R, Cantor A, Muro-Cacho C, Livingston S, Karras J, Pow-Sang J, Jove R. Constitutive activation of STAT3 in human prostate tumors and cell lines: direct inhibition of STAT3 signaling induces apoptosis of prostate cancer cells. Cancer Res. 2002; 62:6659–66. [PubMed: 12438264]
7. Lee SO, Lou W, Hou M, de Migue F, gerber L, Gao AC. Interleukin-6promotes androgen-independent growth in LNCaP human prostate cancer cells. Clin Cancer Res. 2003; 9:370–6. [PubMed: 12538490]
8. Mora LB, Buettner R, Seigne J, et al. Constitutive activation of STAT3 in human prostate tumors and cell lines: Direct inhibition of STAT3 signaling induces apoptosis of prostate cancer cells. Cancer Res. 2002; 62:6659–66. [PubMed: 12438264]
9. Chen T, Wang LH, Farrar WL. Interleukin 6 activates adrogent receptor-mediated gene expression through a signal trasducer and activatior of transcription 3-dependent pathway in LNCaP cancer cells. Cancer Res. 2000; 60:2132–5. [PubMed: 10786674]
10. Trachtenberg J, Blackledge G. Looking to the future. Advances in the management of hormone-refractory prostate cancer. Eur Uorl Suppl. 2002; 1:44–53.
11. Jing N, Tweardy DJ. Targeting STAT3 in cancer therapy. Anti-cancer Drugs. 2005; 16:601–607. [PubMed: 15930886]
12. Jing N, Sha W, Li Y, Xiong W, Tweardy DJ. Rational drug design of G-quartet DNA as anti-cancer agents. Curr Pharma Design. 2005; 11:2841–2854.
13. Henderson, E. Telomere DNA structure. Telomeres: Cold Spring Harbor Laboratory Press; 1995. p. 11-34.
14. Jing N, De Clercq E, Rando FR, Pallansch L, Lackman-Smith C, Lee S, Hogan ME. Stability-activity relationships of a family of G-tetrad forming oligonucleotides as potent HIV inhibitors. J Biol Chem. 2000; 275:3421–30. [PubMed: 10652335]
15. Pilch DS, Plum GE, Breslauer KJ. The thermodynamics of DNA structures that contain lesions or guanine tetrads. Current Opinion Structural Biol. 1995; 5:334–42.
16. Mergny JL, Phan AT, Lacroix L. Following G-quartet formation by UV-spectroscopy. FEBS Letters. 1998; 435:74–8. [PubMed: 9755862]
17. Gou Q, Lu M, Kallenbach NR. Effect of thymine tract length on the structure and stability of model telomeric sequences. Biochemistry. 1993; 32:3596–603. [PubMed: 8466901]
18. Jing N, Xiong W, Guan Y, Pallansch L, Wang S. Potassium dependent folding: a key to intracellular delivery of G-quartet oligonucleotides as HIV inhibitors. Biochemistry. 2002; 41:5397–5403. [PubMed: 11969399]
19. Jing N, Li Y, Xcu X, Li P, Feng L, Tweardy DJ. Targeting STAT3 with G-quartet oligonucleotides in human cancer cells. DNA and Cell Biology. 2003; 22:685–696. [PubMed: 14659041]

20. Jing N, Li Y, Xiong W, Sha W, Jing L, Tweardy DJ. G-quartet oligonucleotides: a new class of STAT3 inhibitors that suppresses growth of prostate and breast tumors through induction of apoptosis. Cancer Res. 2004; 64:6603–9. [PubMed: 15374974]

21. Jing N, Gao XL, Rando FR, Hogan ME. Potassium-induced loop conformation transition of a potent anti-HIV oligonucleotide. J Biomol Struct Dyn. 1997; 15:573–585. [PubMed: 9440003]

22. Jing N, Hogan ME. Structure-activity of tetrad-forming oligonucleotides as a potent anti-HIV therapeutic drug. J Biol Chem. 1998; 273:34992–9. [PubMed: 9857031]

23. Bishop JS, Guy-Caffey JK, Ojwang JO, Smith SR, Hogan ME, Cossum PA, Rando RF, Chaudhary N. G-quartet motifs confer nuclease resistance to a potent anti-HIV oligonucleotide. J Biol Chem. 1996; 271:5698–5703. [PubMed: 8621435]

24. Wallace TL, Gamba-Vitalo C, Loveday KS, Cossum PA. Acute, multiple-dose, and genetic toxicology of AR177, an anti-HIV oligonucleotide. Toxicol Sci. 2000; 53:63–70. [PubMed: 10653522]

25. Jing N, Zhu Q, Yuan P, Li Y, Mao L, Tweardy DJ. Targeting STAT3 with G-quartet oligonucleotides: a potential novel therapy for head and neck cancer. Mol Cancer Therapeutics. 2006; 5:279–286.

26. Weerasinghe P, Garcia GA, Zhu Q, Yuan P, Feng L, Mao L, Jing N. Inhibition of STAT3 activation and tumor growth suppression of non-small cell lung cancer by G-quartet oligonucleotides. Int J Oncology. 2007; 31:129–136.

27. Becker S, Groner B, Muller C. Three-dimensional structure of the STAT3β homodimer bound to DNA. Nature. 1998; 394:145–150. [PubMed: 9671298]

28. Zhu Q, Jing N. Computational Study on Mechanism of G-Quartet Oligodeoxynucleotide Selectively Inhibiting STAT3 Activity. J Computer-aided Mol Design. 2007; 22:641–8.

29. Wallace TL, Gamba-Vitalo C, Loveday KS, Cossum PA. Acute, multiple-dose, and genetic toxicology of AR177, an anti-HIV oligonucleotide. Toxicol Sci. 2000; 53:63–70. [PubMed: 10653522]

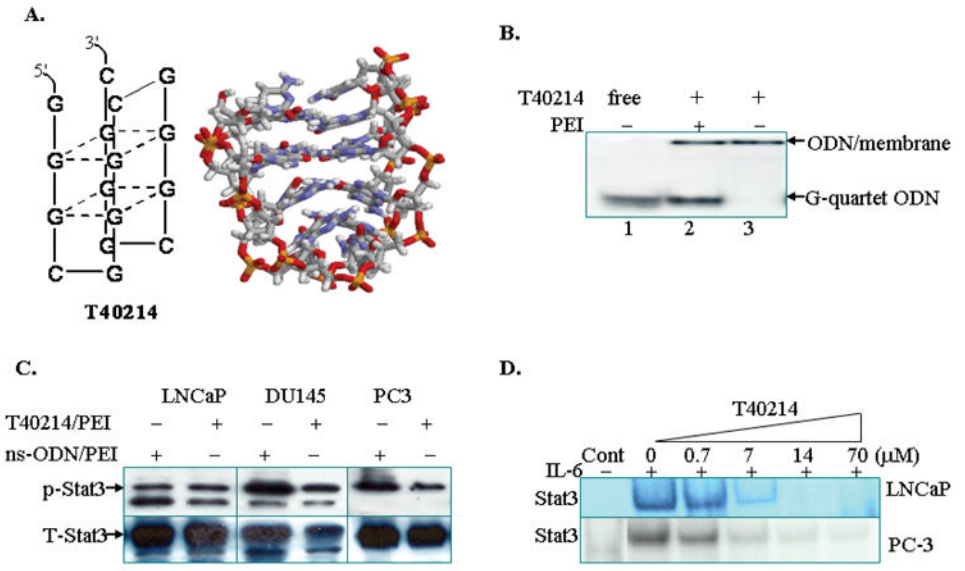

Figure 1.

(A) Structure of T40214; (B) A non-denatured gel demonstrating the structure of T40214. T40214/PEI (Lanes 2) appears as two bands: the higher band corresponds to ODNs adhering on cell membranes (a large sized molecule with slower migration), while the lower band corresponds to the ODNs released inside cells. T40214 in the absence of PEI (Lanes 3) appears as a single, higher, band, indicating that T40214 cannot penetrate cells directly. (C) Western blots showing the expression of p-STAT3 in PC-3, LNCaP or DU145 cells treated with ns-ODN/PEI (14μM) or T40214/PEI (14μM). The expression of total STAT3 (T-STAT3) was used as a control. (D) EMSA showed that T40214 inhibited STAT3 DNA-binding activity (IC_{50}=3μM) in LNCaP and PC-3 cells in a dose-dependent manner.

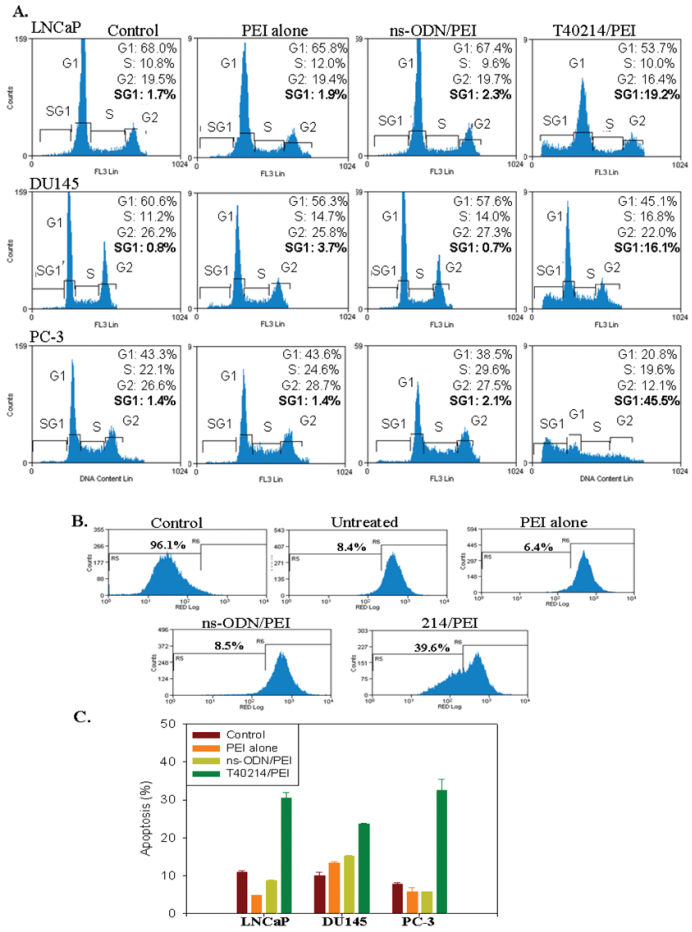

Figure 2.

(A) Cell cycle analyses indicated that T40214 induced apoptosis and arrested cell proliferation in all three prostate cancer cell lines (LNCaP, DU145, PC-3) after exposure to the compound for 24 hours. The fraction of cells in each cell cycle stage or undergoing apoptosis was estimated from the cellular DNA content. Cells in the sub-G1 (SG1) phase have damaged DNA in their nuclei, which results in cell death. (B) Evaluation of the mitochondrial transmembrane potential showed that a positive control affected the mitochondrial potential, and resulted in 96.1% of cells undergoing apoptosis (96.1%). Compared with the percentage of apoptosis in untreated cells (8.4%), the level of apoptosis in PC-3 cells treated with T40214 was increased to 40%. (C) Plots showing the average apoptosis induced by exposure to T40214 in all three prostate cancer cell lines.

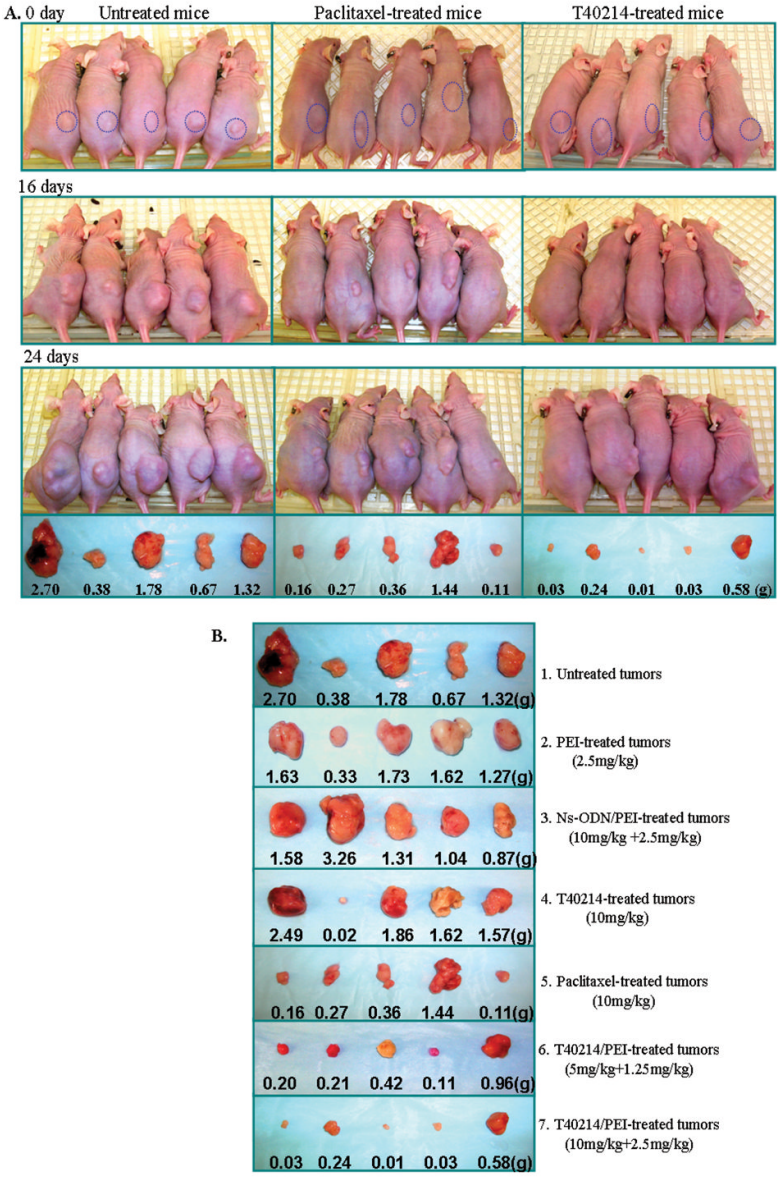

Figure 3.

(A) Tumor growth in nude mice with xenograft prostate tumors treated with paclitexal or T40214/PEI for 0, 16 and 24 days, respectively. (B) Tumor sizes and weights of all five nude mice in the seven groups after 24 days of treatement.

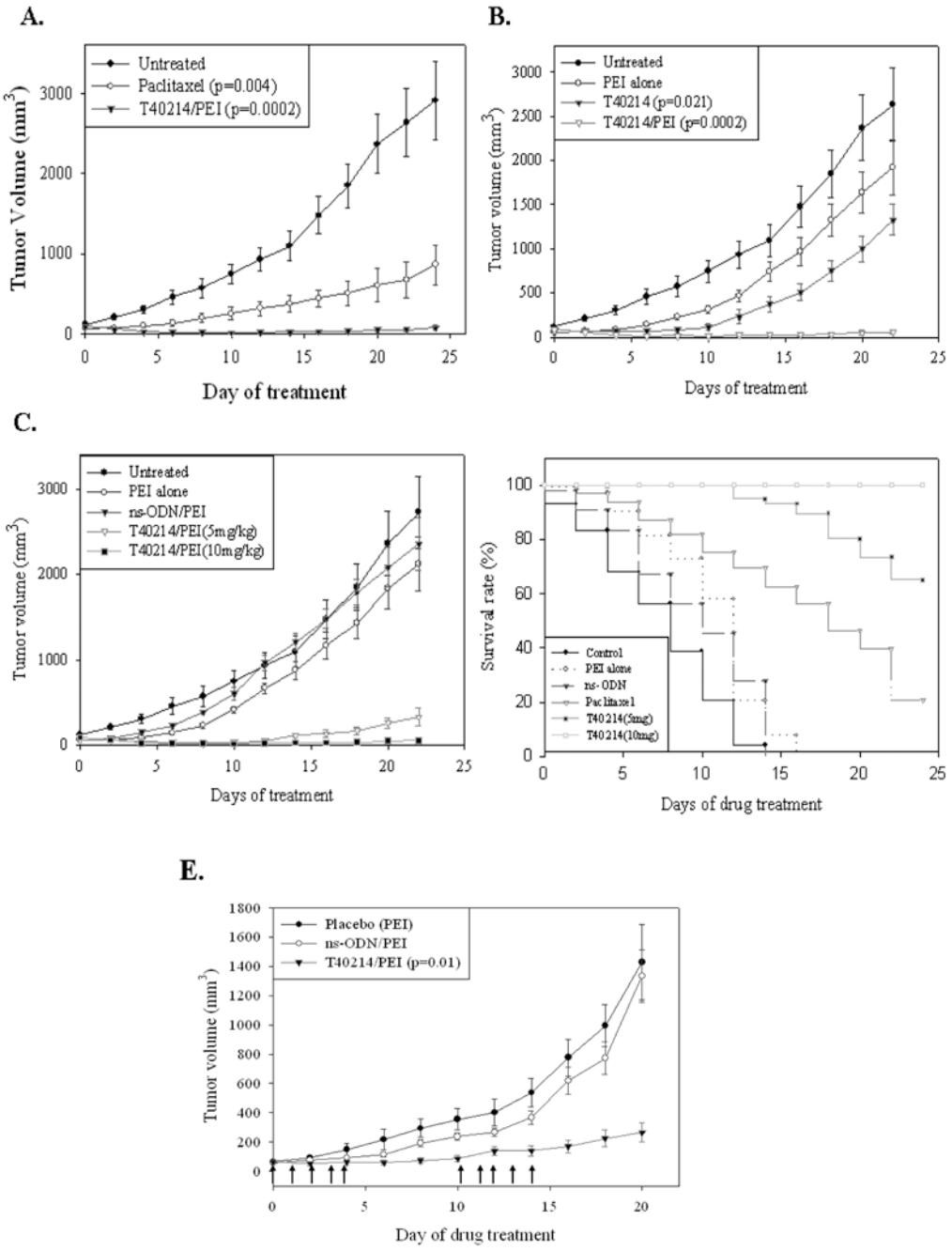

Figure 4.

The effects of the continue treatments on the growth of prostate xenograft tumors (A-C) and the effects of the treatments on animal survival (D). (E) The effects of cyclic treatment on the growth of prostate xenograft tumors. The arrows indicate days that mice received treatment during weeks 1 and 3.

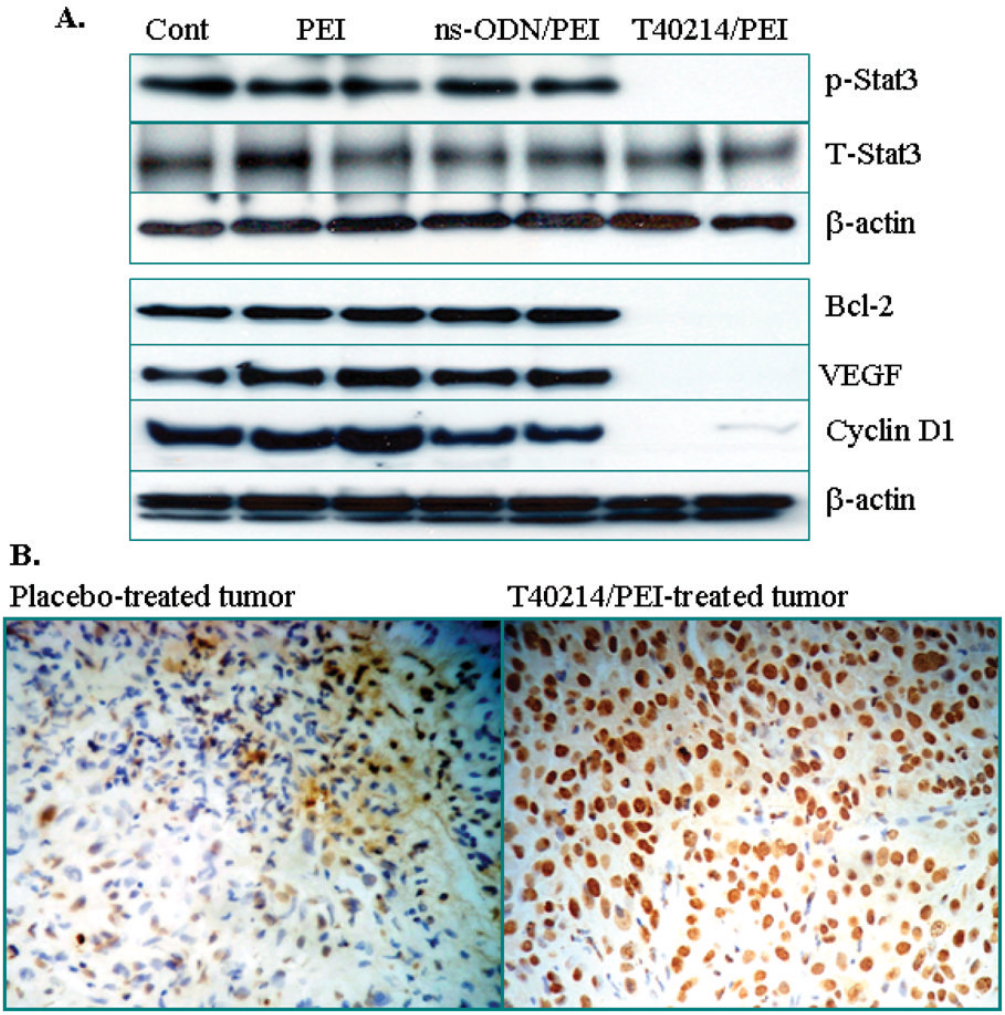

Figure 5.

(A) Western blots of PC-3 tumors after 24-day treatments showed that in tumors, the expression of p-STAT3 and its downstream targets, VEGF, Cyclin D1 and Bcl_2, was suppressed by T40214. (B) Micrographs for apoptotic analysis with 200x magnifications were obtained from tumor tissues of a placebo-treated mouse (left panel) and a T40214-treated mouse (right panel) under the same experimental conditions. The apoptotic tumor cells were stained brown by TUNEL-positive staining, while the normal (non-apoptotic) tumor cells remained blue (negative staining for TUNEL).

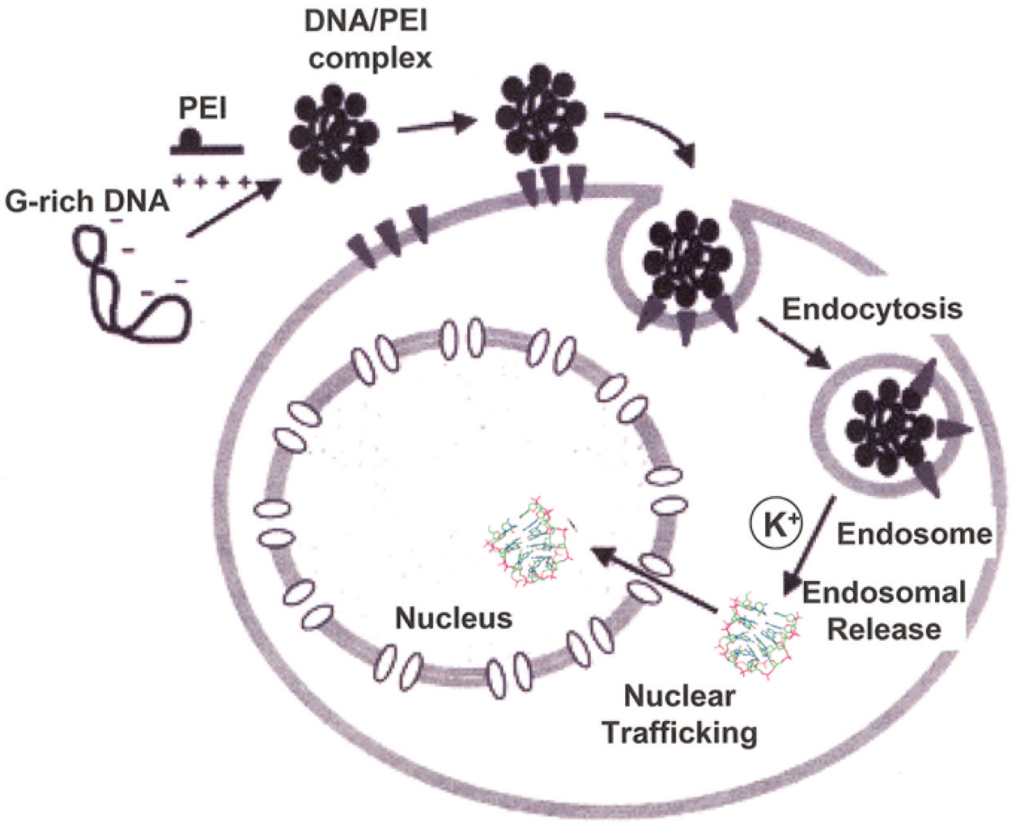

Figure 6.
A cartoon depicting the intracellular delivery system developed for GQ-ODN T40214 using PEI as a vehicle (18).

Table 1

In vivo effects of T40214/PEI against PC-3 xenograft tumors in nude mice

Group	Drug dose	No. of mice		Weight of mice (g)		Tumor (mm^3)		Fold of tumor-growth	Mean-tumor weight (g)	P value
		Start	End	Start	End	Start	End			
Control	untreated	5	5	27.2±1.5	25.2±1.7	93.1 ± 25	2633 ± 657	41.20 ± 9.30	1.37 ± 0.37	
PEI alone	3.75mg/kg	5	5	24.9±1.7	23.7±1.2	58.3 ± 7.9	1924 ± 374	40.85 ± 7.95	1.32 ± 0.58	-----
ns-ODN/PEI	5mg/kg+1.25mg/kg	5	5	27.2±1.5	22.3±1.6	67.9 ± 12	2362 ± 565	40.79 ± 9.75	1.61 ± 0.38	-----
T40214	10mg/kg	5	5	25.1±0.5	22.2±1.9	55.7 ± 4.9	1327 ± 333	23.82 ± 5.97	1.50 ± 0.40	-----
Paclitexal	10mg/kg	5	5	18.6±1.0	20.6±1.0	70.7 ± 7.3	672 ± 300	9.50 ± 5.67	0.47 ± 0.22	<0.005
T40214/PEI	5mg/kg+1.25mg/kg	5	5	25.5±0.7	26.8±1.5	72.9 ± 8.3	329 ± 147	5.15 ± 2.31	0.38 ± 0.14	<0.001
T40214/PEI	10mg/kg+2.5mg/kg	5	5	25.3±1.1	26.5±1.6	91.0 ± 16	55 ± 38	0.61 ± 0.41	0.18 ± 0.10	<0.0005